Chemistry–A European Journal
Research Article
doi.org/10.1002/chem.202203663
Chemistry Europe
European Chemical Societies Publishing
www.chemeurj.org

C–C and C–N Bond Activation, Lewis-Base Coordination and One- and Two-Electron Oxidation at a Linear Aminoborylene

Robert Witte,[a, b] Merle Arrowsmith,[a, b] Anna Lamprecht,[a, b] Fabian Schorr,[a, b] Ivo Krummenacher,[a, b] and Holger Braunschweig*[a, b]

Abstract: A cyclic alkyl(amino)carbene (CAAC)-stabilized dicoordinate aminoborylene is synthesized by the twofold reduction of a [(CAAC)BCl_2(TMP)] (TMP = 2,6-tetramethylpiperidyl) precursor. NMR-spectroscopic, X-ray crystallographic and computational analyses confirm the cumulenic nature of the central C=B=N moiety. Irradiation of [(CAAC)B(TMP)] (**2**) resulted in an intramolecular C–C bond activation, leading to a doubly-fused $C_{10}BN$ heterocycle, while the reaction with acetonitrile resulted in an aryl migration from the CAAC to the acetonitrile nitrogen atom, concomitant with tautomerization of the latter to a boron-bound allylamino ligand. One-electron oxidation of **2** with CuX (X=Cl, Br) afforded the corresponding amino(halo)boryl radicals, which were characterized by EPR spectroscopy and DFT calculations. Placing **2** under an atmosphere of CO afforded the tricoordinate (CAAC,CO)-stabilized aminoborylene. Finally, the twofold oxidation of **2** with chalcogens led, in the case of N_2O and sulfur, to the splitting of the B–C_{CAAC} bond and formation of the 2,4-diamino-1,3,2,4-dichalcogenadiboretanes and CAAC-chalcogen adducts, whereas with selenium a monomeric boraselenone was isolated, which showed some degree of B–Se multiple bonding.

Introduction

The stabilization of low-valent borylenes (BR, R = anionic substituent) has generated much research interest since the isolation of the first transition metal borylene complexes in the 1990s.[1] The challenge of synthesizing these reactive boron(I) compounds lies in the presence of the two vacant p orbitals at boron, combined with a highly nucleophilic lone pair. Thus, free borylenes such as :BH, :BF or :BPh may only be observed transiently or evidenced by trapping reactions.[2–4] Transition metal complexes provided the first entry point into the isolation of stable borylenes, as the d orbitals of electron-rich metals act as powerful donors to the empty p orbital at boron and acceptors to the boron lone pair.[5–7] A landmark in this area was the isolation of the first linear metal borylene complexes **I** (Figure 1), in which the second empty orbital at boron is additionally stabilized by π donation and steric protection from the bis(trimethylsilyl)amino substituent.[8,9] While terminal metal borylene complexes proved useful as borylene transfer reagents,[10] the dearth of substituents R capable of stabilizing the linear M=B–R motif remained a serious limitation.

The first stable metal-free borylene, synthesized in 2010 by Bertrand,[11] relied on the electronic and steric stabilization of two cyclic alkyl(amino)carbene (CAAC) ligands, acting as strong σ donors and π acceptors,[12,13] and thus enabling the delocalization of the excess electron density over the entire CAAC–B–CAAC π framework. Since then, numerous symmetrical and unsymmetrical tricoordinate borylene derivatives (LL′BR, L,L′ = neutral donor ligands) with various R substituents (e.g., H, F, Cl, Br, CN, NCS, aryl, boryl) have been isolated.[14,15] Their reactivity, however, remains often hampered by excessive steric hindrance around the tricoordinate boron center. While

[a] R. Witte, Dr. M. Arrowsmith, A. Lamprecht, Dr. F. Schorr, Dr. I. Krummenacher, Prof. Dr. H. Braunschweig
Institute for Inorganic Chemistry
Julius-Maximilians-Universität Würzburg
Am Hubland, 97074 Würzburg (Germany)
E-mail: h.braunschweig@uni-wuerzburg.de

[b] R. Witte, Dr. M. Arrowsmith, A. Lamprecht, Dr. F. Schorr, Dr. I. Krummenacher, Prof. Dr. H. Braunschweig
Institute for Sustainable Chemistry & Catalysis with Boron
Julius-Maximilians-Universität Würzburg
Am Hubland, 97074 Würzburg (Germany)

Supporting information for this article is available on the WWW under https://doi.org/10.1002/chem.202203663

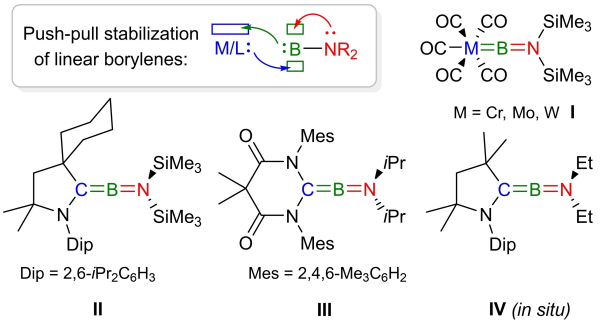

Figure 1. Examples of literature-known sp^2-hybridized aminoborylenes.

dicoordinate metal-free borylenes (LBR) can be generated in situ by photolysis or thermolysis of a second labile donor ligand (e.g., CO, PMe_3), they are too reactive to isolate, undergoing systematic intramolecular C–H or C–C bond activation in the absence of a second stabilizing base.[16–22]

The first stable linear metal-free borylene, compound **II**, relied on a similar push-pull principle as the linear metal aminoborylenes, the σ-donating and π-acidic $CAAC^{Cy}$ ligand playing the role of the transition metal and the amino substituent affording the additional electronic and steric stabilization.[23] While the C–B–N bonding situation in the solid-state structure of **II** is best described as allenic, calculations showed that bending of the C–B–N angle, which comes at a negligible energetic cost, localizes the lone pair at boron, allowing it to react in the manner of a borylene. The only other isolated dicoordinate borylene, compound **III**, was designed on the same principle using a diamidocarbene (DAC) instead of a CAAC ligand.[24,25] More recently, our group has reported the in situ synthesis of the much less sterically hindered linear aminoborylene **IV**, which was only stable in solution at temperatures below −40 °C and could be trapped as a CO adduct.[26] Furthermore, we have synthesized aminoborylene-stabilized aminoborylenes in the coordination sphere of transition metal carbonyls, with side-on coordination of the B–B multiple bond to the metal center, in which the terminal aminoborylene moiety is also partially sp-hybridized.[27] In terms of reactivity, however, only two reactions have ever been reported for linear aminoborylenes, namely the coordination of CO and the activation of H_2 across the C_{CAAC}–B bond.[23,26]

In this study we describe the synthesis and characterization of a new isolable CAAC-stabilized aminoborylene with lower steric hindrance at boron than **II** and describe its C–C and C–N bond activation chemistry, its one-electron oxidation to the corresponding amino(halo)boryl radicals, its binding to CO and finally its two-electron oxidation with elemental chalcogens.

Results and Discussion

The addition of $CAAC^{Me}$ (1-(2,6-di*iso*propylphenyl)-3,3,5,5-tetramethylpyrrolidin-2-ylidene)[28] to $(TMP)BCl_2$ (TMP = 2,6-tetramethylpiperidyl) in pentane at room temperature afforded the corresponding adduct **1** in quantitative yield (Scheme 1a). Once redissolved in C_6D_6 at room temperature, however, the adduct redissociated into the starting materials, as indicated by the ^{11}B NMR shift at 33.3 ppm, corresponding to free $(TMP)BCl_2$.[29] A variable-temperature ^{11}B NMR experiment in d_8-toluene showed the appearance of another resonance at 4.5 ppm attributable to adduct **1** at temperatures below 0 °C (see Figure S19 in the Supporting Information).

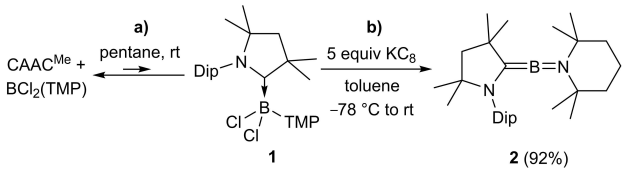

Scheme 1. Synthesis of aminoborylene **2**.

The reduction of crude **1** with 5 equiv. KC_8 in toluene yielded a red suspension, workup of which afforded the linear aminoborylene **2** as a dark orange solid in 92% yield (Scheme 1b). The UV-vis spectrum of **2** in hexane shows an absorption maximum at 246 nm and a broad, very low intensity absorption band at 353 nm. The ^{11}B NMR spectrum of **2** shows a broad resonance at 71.7 ppm (full width at mid-height (fwmh) ≈570 Hz), intermediate between the linear aminoborylenes of Bertrand and Stephan (**II** δ_{11B} = 83.7 ppm)[23] and Hudnall (**III** δ_{11B} = 62 ppm),[24] and similar to that observed in situ for **IV** (δ_{11B} = 73 ppm).[26] The CAAC carbene carbon was detected as a very broad $^{13}C\{^1H\}$ NMR resonance at 115.2 ppm, downfield from known aminoboraalkenes (δ_{11B} = 69–89 ppm),[30–32] which display a covalent B=C double bond, but significantly upfield from typical BC_{CAAC} resonances of CAAC-stabilized borylenes (δ_{11B} = 154–204 ppm).[33–36] An X-ray crystallographic analysis (Figure 2a) confirmed the near-linear aminoboraalkene conformation of the C=B=N moiety (170.91(11)°) and the double bond character of the C1–B1 (1.4078(15) Å) and B1–N2 (1.3662(14) Å) bonds, similar to those in **II** and **III** (**II**: B–C 1.401(5), B–N 1.382(5) Å; **III**: B–C 1.416(3) Å).[25] The TMP ligand is rotated so as to minimize steric repulsion between the TMP methyl and the $CAAC^{Me}$ methyl and Dip substituents, with an angle of ca. 60° between the C1 and N2 planes. The lower steric demands of the $CAAC^{Me}$ and TMP ligand of **2** compared to those of the $CAAC^{Cy}$ and $N(SiMe_3)_2$ ligands of **II** are expected to provide a more reactive borylene center in **2**. Shortly after the submission of this manuscript Chiu and coworkers reported the first linear boryl radical cation, $[(CAAC^{Cy})B(TMP)]^{\bullet+}$, which like **2** is stabilized by the push-pull interaction of a CAAC and a TMP ligand, but

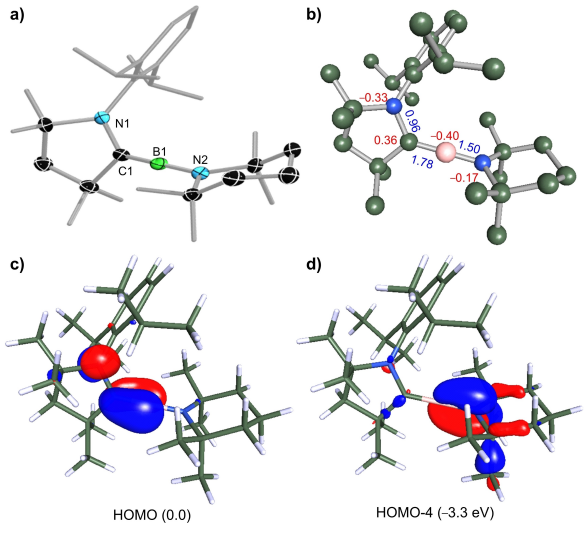

Figure 2. a) X-ray crystallographically-derived solid-state structure of **2**, with atomic displacement ellipsoids shown at the 50% probability level. All hydrogen atoms and ellipsoids of ligand periphery are omitted for clarity. b) Optimized structure of **2** at the B3LYP-D3(BJ)-Def2-SVP level of theory, with relevant Wiberg bond indexes (WBIs) in blue and Mulliken partial charges in red. c and d) Representation of the HOMO and HOMO-4 of **2**, relative energy levels (eV) in parentheses. Isosurfaces: 0.06.

with a slightly longer B–C (1.457(3) Å) and slightly shorter B–N (1.347(3) Å) bonds.[37]

Density functional theory (DFT) calculations at the B3LYP–D3(BJ)-def2-SVP level of theory (see the Supporting Information for computational details) provide similar structural parameters to those of the solid-state structure (B–C 1.41, B–N 1.37 Å, C–B–N 177°). The highest occupied molecular orbital (HOMO) corresponds to the B=C π bond with an out-of-phase contribution of the CAAC nitrogen p_z orbital (Figure 2c), as was also calculated for **II** and **III**.[23,24] The B–N π bond is visible in the HOMO-4 (Figure 2d). The calculated Wiberg bond indexes (WBIs) of the B–C and B–N bonds of 1.78 and 1.50, respectively, confirm their partial double bond character (Figure 2b). Finally, the partial charge of −0.40 at boron is consistent with a highly nucleophilic borylene center.

Irradiation of a hexane solution with UV light for 7 days resulted in selective activation of a C_{Ar}–C_{iPr} bond by the borylene center of **2**, followed by *i*Pr transfer from boron to the CAAC carbene center, yielding the doubly-fused B,N-heterocycle **3** (Scheme 2a).[38] The same decomposition was also observed for aminoborylene **IV** upon warming to room temperature.[26] This seems to be a feature particular to dicoordinate CAAC-stabilized aminoborylenes, since in situ-generated dicoordinate CAAC-stabilized arylborylenes instead undergo insertion of the borylene into the C–H bond of an *i*Pr-methyl group of the Dip substituent, often followed by hydride transfer from boron to the CAAC carbene center.[16,36,39]

Intramolecular borylene insertion into a C_{Ar}–C_{iPr} bond without further migration of the *i*Pr moiety has been observed with in situ-generated dicoordinate mesoionic carbene- and isocyanide-stabilized arylborylenes.[18,19] The solid-state structure of **3** confirms the formal addition of the C_{Ar}–C_{iPr} bond across the B–C_{CAAC} bond (Figure 3, left) and the formation of fused tricyclic system with a central 2-hydro-1,3-azaborole ring. It is noteworthy that, due to the bulk of the TMP ligand, the planes of the B2 and N2 centers in **3** form an angle of 42° rather than being quasi-coplanar as in the diethylamino analogue of **3**.[26] This leads to a lower degree of π overlap between the nitrogen lone pair and the empty orbital at boron, a lengthening of the B–N bond to 1.438(2) Å (vs. 1.397(2) Å in the diethylamino analogue), which results in a 10 ppm downfield shift of the ^{11}B NMR resonance of **3** at 53.8 ppm compared to the diethylamino analogue (δ_{11B} = 43 ppm).[26]

In acetonitrile borylene **2** underwent quantitative transfer of the Dip substituent from the CAAC to the acetonitrile nitrogen atom, concomitant with tautomerization of the acetonitrile CMe moiety to a vinyl group, resulting in the pyrrolidin-2-yl and aryl(vinyl)amino-substituted borane **4** (Scheme 2b). Compound **4** displays an ^{11}B NMR resonance at 36.6 ppm, typical for an alkyl(diamino)borane (e.g., $MeB(NMe_2)_2$ δ_{11B} = 33.5 ppm).[40] The ^{1}H NMR spectrum shows a characteristic set of three vinylamino resonances in a 1:1:1 ratio at 8.01 (dd, NC*H*), 4.35 (d, H_{cis}) and 3.81 (d, H_{trans}) ppm, with $^3J_{cis}$ and $^3J_{trans}$ coupling constants of 8.9 and 16.1 Hz, respectively. The solid-state structure of **9** (Figure 5) confirms the migration of the Dip substituent from N1 to N3, as well as the tautomerization of the CMe to the allyl substituent, with a C2–C3 double bond of 1.324(4) Å. Migration of the Dip substituent from the CAAC nitrogen to the carbon atom of a boron-bound ligand has only been observed within the radical anion $[(CAAC^{Me})B(CO)(Tip)]^{\bullet-}$ (Tip = 2,4,6-tri*iso*propylphenyl).[41] The reaction likely proceeds via the formation of a tricoordinate acetonitrile adduct **A**, followed by tautomerization to a CAAC-stabilized amino(vinylimino)borane

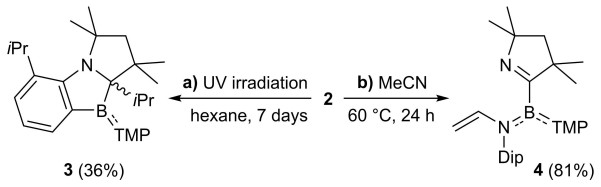

Scheme 2. C–C and C–N bond activation at **2**.

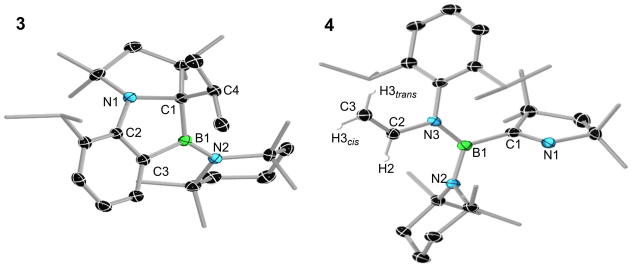

Figure 3. X-ray crystallographically-derived solid-state structures of **3** and **4**, with atomic displacement ellipsoids shown at the 50% probability level. All hydrogen atoms and ellipsoids of ligand periphery are omitted for clarity, except for the vinyl protons.

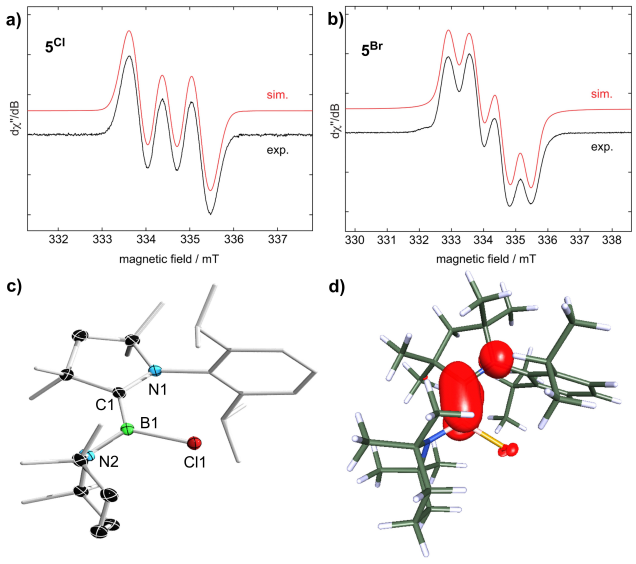

Figure 4. a, b) Experimental (black) and simulated (red) continuous-wave (CW) X-band EPR spectra of 5^{Cl} (a) and 5^{Br} (b) in THF at room temperature; c) X-ray crystallographically-derived solid-state structures of 5^{Cl}, with atomic displacement ellipsoids shown at the 50% probability level. All hydrogen atoms and ellipsoids of ligand periphery are omitted for clarity, except for the allyl protons; d) Plots of the spin density of 5^{Cl} and 5^{Br} calculated at the B3LYP-D3(BJ)-def2-SVP level of theory (doublet states). Isosurfaces: 0.004. Localization of unpaired electron for 5^{Cl}: N 0.25, C 0.44, B 0.27, Cl 0.02.

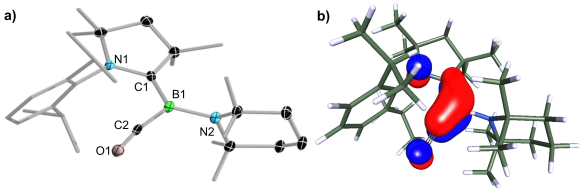

Figure 5. a) X-ray crystallographically-derived solid-state structure of **6**, with atomic displacement ellipsoids shown at the 50% probability level. All hydrogen atoms and ellipsoids of ligand periphery are omitted for clarity. b) Representation of the HOMO of **6** at the B3LYP-D3(BJ)-Def2-SVP level of theory. Isosurfaces: 0.06.

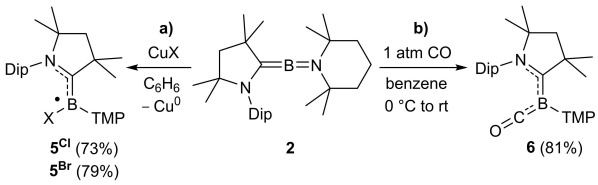

Scheme 4. One-electron oxidation of **2** and adduct formation with CO.

B and finally Dip migration from the CAAC to the imino nitrogen atom (Scheme 3).

The one-electron oxidation of **2** with copper chloride or bromide afforded the red-colored, NMR-silent boryl radicals $\mathbf{5^{Cl}}$ and $\mathbf{5^{Br}}$ (Scheme 4a). The UV-vis spectra of $\mathbf{5^{Cl}}$ and $\mathbf{5^{Br}}$ show absorption maxima at 321 and 327 nm, respectively, with a low-absorption shoulder around 500 nm, accounting for their red color. The EPR spectrum of $\mathbf{5^{Cl}}$ shows a broad triplet at $g_{iso}=2.0037$, which could be modelled with hyperfine coupling constants of $a(^{14}N_{CAAC})=18.9$ MHz, $a(^{11}B)=3.1$ MHz, $a(^{14}N_{TMP})=2.8$ MHz and $a(^{36,39}Cl)=1.2$ MHz (Figure 4a). This suggests that the unpaired electron is delocalized over the entire (CAAC^{Me})BCl(TMP) π framework with the highest contribution at the CAAC nitrogen. In their very recent publication Chiu and coworkers reported the synthesis of the CAAC^{Cy} analogue of $\mathbf{5^{Cl}}$ by the reduction of a [(CAAC^{Cy})BCl(TMP)][OTf] (Tf=SO_2CF_3) precursor, and also obtained an EPR triplet resonance.[37] A similar hyperfine coupling pattern has been observed for the chloroboryl radical precursor to **II** and [(CAAC)B(Cl)N(SiMe$_3$)$_2$]$^{-\cdot}$.[23,26] In contrast, the chloroboryl radical precursor to **III** showed much larger coupling to the chlorine nucleus ($a(^{35}Cl)=24.5$ MHz).[24] The EPR spectrum of $\mathbf{5^{Br}}$ shows a broad quartet at $g_{iso}=2.0075$, which could be modelled with hyperfine coupling constants of $a(^{14}N_{CAAC})=19.0$ MHz, $a(^{11}B)=2.1$ MHz, $a(^{14}N_{TMP})=3.4$ MHz and $a(^{79,81}Br)=8.4$ MHz (Figure 4b). These values are similar to those observed for the related bromoboryl radical [(CAAC^{Me})B(Br)Dur]$^{\bullet}$ (Dur = 2,3,5,6-tetramethylphenyl).[42] DFT calculations show that the spin density in both cases is mainly delocalized over the (N–C)$_{CAAC}$-B π framework ($\mathbf{5^{Cl}}$: N 0.25, C 0.44, B 0.27; $\mathbf{5^{Br}}$: N 0.26, C 0.42, B 0.29) with minimal contributions from the halide ligand (Figure 4d and Figure S27 in the Supporting Information). Compared to other CAAC-stabilized boryl radicals $\mathbf{5^{Cl}}$ and $\mathbf{5^{Br}}$ show a similar distribution of the unpaired electron spin density.[37,43]

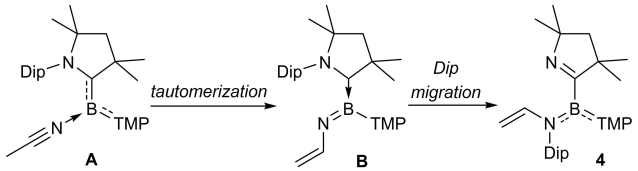

Scheme 3. Proposed mechanism for the formation of **4**.

The solid-state structures of $\mathbf{5^{Cl}}$ and $\mathbf{5^{Br}}$ show the typical structural features of CAAC-stabilized boryl radicals:[23,26,42,43] the boron center is trigonal planar ($\Sigma_{\angle B}\approx360°$), the B–$C_{CAAC}$ bond ($\mathbf{5^{Cl}}$ 1.5181(19); $\mathbf{5^{Br}}$ 1.513(2) Å) longer and the C1–N1 bond ($\mathbf{5^{Cl}}$ 1.3815(16); $\mathbf{5^{Br}}$ 1.3759(17) Å) shorter than those of borylene **2** (B1–C1 1.4078(15), N1–C1 1.4255(13) Å), thus confirming the delocalization of the unpaired electron over the B–C–N π framework.

Like the linear aminoborylenes **II** and **IV**[23,26] compound **2** reacted with CO to form the tricoordinate borylene **6** (Scheme 4b). The ^{11}B NMR shift at −5.8 ppm is slightly upfield-shifted from that of the CO adducts of **II** ($\delta_{11B}=-3.4$ ppm)[23] and **IV** ($\delta_{11B}=-2.7$ ppm),[26] indicating a higher electron density at boron. The highly broadened $^{13}C\{^1H\}$ NMR resonance of the boron-bound C_{CAAC} nucleus was detected by HMBC at 203.0 ppm, while the BCO resonance could not be detected. The IR C≡O stretching frequency of **6** appears as a strong band at 1925 cm^{-1}, close to that of (CAAC^{Me})B(CO)NEt$_2$ ($\nu_{CO}=1928$ cm^{-1}).[26] The solid-state structure of **6** confirms the formation of the CO adduct (Figure 5). The CO ligand is nearly coplanar with the CAAC π framework (torsion angle N1–C1–B1–C2 9.8(6)°) and oriented toward the NDip residue. The B–C_{CAAC} and B–C_{CO} distances of 1.508(6) and 1.494(6) Å, respectively, are within the range of partial double bonds, as is usual for (CAAC,CO)-stabilized borylenes,[16,23,42–47] whereas the B–N_{TMP} bond (1.510(5) Å) is now best described as a single bond.

DFT calculations show that the HOMO of **4** is delocalized over the N_{CAAC}–C–B–C–O π framework, with bonding interactions over the C_{CAAC}–B–C_{CO} moiety and out-of-phase contributions of the CAAC nitrogen and carbonyl oxygen atoms. The calculated WBIs for the N1–C1 (1.20), C1–B1 (1.39), B1–C2 (1.33) and C2–O1 (2.16) bonds confirm the delocalization of the π electrons, while the WBI for B1–N2 (1.06) is indicative of a single rather than a partial double bond.

As tricoordinate borylenes are known to activate elemental chalcogens,[48–50] borylene **2** was reacted with N_2O, typically used as a selective oxygen source in reactions with silylenes,[51] as well as elemental sulfur and selenium. With both N_2O and sulfur, the B–C_{CAAC} bond was cleaved and the boron and carbene centers fully oxidized, leading to the quantitative formation of a 2:1 mixture of the known CAAC-chalcogen adducts **7°** and **7^S**, respectively,[52,53] and the known 2,4-diamino-1,3,2,4-dichalcogenadiboretanes **8°** ($\delta_{11B}=28.2$ ppm) and **8^S** ($\delta_{11B}=40.7$ ppm), respectively,[54,55] as identified by NMR spectroscopic and X-ray crystallographic analyses (Scheme 5a). A similar complete oxidation of (CAAC^{Me})$_2$Si with N_2O, yielding

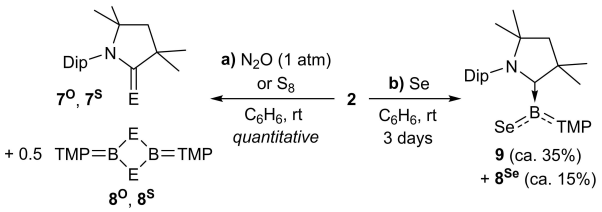

Scheme 5. Reactivity of **2** towards elemental chalcogen sources.

7° and SiO_2, has been reported by Roesky and Stalke.[56] In the reactions of **2** with N_2O and S_8 it is likely that the first oxidation occurs at the borylene center, yielding a monomeric (CAAC^{Me})B=E(TMP) (E=O, S) intermediate with a labile CAAC ligand, followed by oxidation of the CAAC ligand and dimerization of the kinetically unstable B=E(TMP) residue. The reaction with elemental selenium proved less selective, leading to incomplete conversion even after prolonged reaction times at room temperature.[57] The major product formed (ca. 35%) shows an ^{11}B NMR resonance at 44.4 ppm and was identified by X-ray crystallographic analysis as the boraselenone **9** (Scheme 5b).[58] The ^{1}H NMR spectrum of **9** shows very broad CAAC resonances, indicative of strongly hindered rotation. The second product, formed in ca. 15% yield, was the known 1,3,2,4-diselenadiboretane **8^{Se}** (δ_{11B} = 34.5 ppm),[54] while three minor byproducts (δ_{11B} = 48.6, 30.3 and 25.4 ppm, each less than 2%) remained unidentified.

The solid-state structure of **9** (Figure 6a) shows a trigonal planar boron center (Σ(∠B) = 359.5(3)°) with a very narrow C–B–Se angle of 90.5(3)° and very wide Se–B–N and N–B–C angles of 133.1(3) and 135.9(4)°, respectively. This results in a relatively short Se···C_{CAAC} distance of 2.52 Å, just below the limit of the sum of van der Waals radii for carbon and selenium (2.60 Å),[58] suggesting a possible orbital interaction. This was confirmed by DFT calculations, which provide a C–B–Se angle of 88.9° and a Se···C_{CAAC} distance of 2.47 Å, and show that the HOMO-1 is composed of the second lone pair at selenium donating into the empty p_z orbital at the carbene center (Figure 6d). Furthermore, the selenium atom lies in the plane of the amino substituent (torsion angle Se1–B1–N2–C2 0.9(6)°), whereas the CAAC ligand is rotated near-orthogonally to the boron plane (N1–C1–B1–Se1 −88.4(4)°). This results in a purely σ-donating CAAC→B interaction, with a C1–B1 single bond (1.599(6) Å). The B1–N2 bond length of 1.415(6) Å indicates partial double bond character, while the B1–Se1 bond (1.927(5) Å) is longer than that in known boraselenones with authenticated B=Se double bonds (1.871(5)–1.896(4) Å).[49,60,61] Inspection of the HOMOs of **9** shows that, while the HOMO and HOMO-1 are essentially the two lone pairs at selenium and the HOMO-5 corresponds to the B–Se σ bond, the HOMO-3 shows delocalized Se-B–N π-bonding character (Figure 6c–f). The WBIs of the B–Se (1.21) and B–N bonds (1.37) also confirm their partial double bond character, while the negative charge at selenium (−0.37) and much less negative charge at boron (−0.05) suggest that the boraselenolate form is still electronically predominant (Figure 6b).

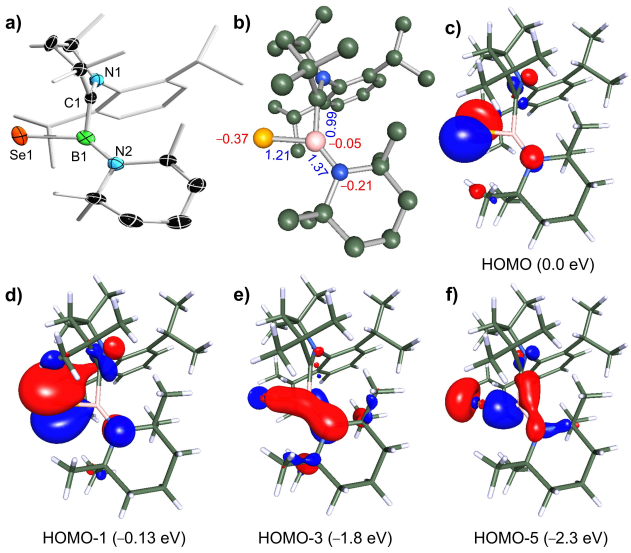

Figure 6. a) X-ray crystallographically-derived solid-state structure of **9**, with atomic displacement ellipsoids shown at the 50% probability level. All hydrogen atoms and ellipsoids of ligand periphery are omitted for clarity. b) Optimized structure of **9** at the B3LYP-D3(BJ)-Def2-SVP level of theory, with relevant WBIs in blue and Mulliken partial charges in red. c–f) Representation of selected HOMOs of **9**, relative energy levels (eV) in parentheses. Isosurfaces: 0.06.

Conclusion

We have synthesized the third isolable linear aminoborylene, compound **2**, stabilized by the push-pull interaction of a π-donating piperidyl and a π-accepting CAAC ligand. While structural and computational analyses confirm its cumulenic C=B=N structure, its reactivity is that expected for a dicoordinate borylene, including intramolecular C–C and N–C bond activation reactions, one-electron oxidation to amino(halo)boryl radicals and the binding of CO and elemental selenium.

Experimental Section

All experimental details provided in the Supporting Information in a separate file (pdf): synthetic procedures, NMR, IR, UV-vis, EPR and X-ray crystallographic data, as well as details of the computations.

Crystallographic data: Deposition Number(s) 2221458 (**9**), 2221459 (**6**), 2221460 (**1**), 2221461 (**5^{Cl}**), 2221462 (**5^{Br}**), 2221463 (**4**), 2221464 (**2**) and 2221465 (**3**) contain(s) the supplementary crystallographic data for this paper. These data are provided free of charge by the joint Cambridge Crystallographic Data Centre and Fachinformationszentrum Karlsruhe Access Structures service.

Acknowledgements

The authors thank the Deutsche Forschungsgemeinschaft (project numbers BR1149/22-1 and 466754611) for funding. Open Access funding enabled and organized by Projekt DEAL.

Conflict of Interest

The authors declare no conflict of interest.

Data Availability Statement

The data that support the findings of this study are available from the corresponding author upon reasonable request.

Keywords: bond activation · boraselenone · dicoordinate borylene · one-electron oxidation · push-pull stabilization

[1] D. Vidovic, G. A. Pierce, S. Aldridge, *Chem. Commun.* **2009**, 1157–1171.
[2] W. Lochte-Holtgreven, E. S. van der Vleugel, *Z. Phys.* **1931**, *70*, 188–203.
[3] P. L. Timms, *J. Am. Chem. Soc.* **1967**, *89*, 1629–1632.
[4] H. F. Bettinger, *J. Am. Chem. Soc.* **2006**, *128*, 2534–2535.
[5] J. T. Goettel, H. Braunschweig, *Coord. Chem. Rev.* **2019**, *380*, 184–200.
[6] H. Braunschweig, R. D. Dewhurst, V. H. Gessner, *Chem. Soc. Rev.* **2013**, *42*, 3197–3208.
[7] D. Vidovic, S. Aldridge, *Chem. Sci.* **2011**, *2*, 601–608.
[8] A. H. Cowley, V. Lomelí, A. Voigt, *J. Am. Chem. Soc.* **1998**, *120*, 6401–6402.
[9] H. Braunschweig, C. Kollann, U. Englert, *Angew. Chem. Int. Ed.* **1998**, *37*, 3179–3180; *Angew. Chem.* **1998**, *110*, 3355–3357.
[10] C. E. Anderson, H. Braunschweig, R. D. Dewhurst, *Organometallics* **2008**, *27*, 6381–6389.
[11] R. Kinjo, B. Donnadieu, M. A. Celik, G. Frenking, G. Bertrand, *Science* **2011**, *333*, 610–613.
[12] S. K. Kushvaha, A. Mishra, H. W. Roesky, K. C. Mondal, *Chem. Asian J.* **2022**, e202101301.
[13] M. Melaimi, R. Jazzar, M. Soleilhavoup, G. Bertrand, *Angew. Chem. Int. Ed.* **2017**, *56*, 10046–10068; *Angew. Chem.* **2017**, *129*, 10180–10203.
[14] M.-A. Légaré, C. Pranckevicius, H. Braunschweig, *Chem. Rev.* **2019**, *119*, 8231–8261.
[15] M. Soleilhavoup, G. Bertrand, *Angew. Chem. Int. Ed.* **2017**, *56*, 10282–10292; *Angew. Chem.* **2017**, *129*, 10416–10426.
[16] H. Braunschweig, I. Krummenacher, M.-A. Légaré, A. Matler, K. Radacki, Q. Ye, *J. Am. Chem. Soc.* **2017**, *139*, 1802–1805.
[17] C. Pranckevicius, J. O. C. Jiménez-Halla, M. Kirsch, I. Krummenacher, H. Braunschweig, *J. Am. Chem. Soc.* **2018**, *140*, 10524–10529.
[18] M. Arrowsmith, J. Böhnke, H. Braunschweig, H. Gao, M.-A. Légaré, V. Paprocki, J. Seufert, *Chem. Eur. J.* **2017**, *23*, 12210–12217.
[19] H. Braunschweig, R. D. Dewhurst, F. Hupp, M. Nutz, K. Radacki, C. W. Tate, A. Vargas, Q. Ye, *Nature* **2015**, *522*, 327–330.
[20] D. P. Curran, A. Boussonniere, S. J. Geib, E. Lacote, *Angew. Chem. Int. Ed.* **2012**, *51*, 1602–1605; *Angew. Chem.* **2012**, *124*, 1634–1637.
[21] P. Bissinger, H. Braunschweig, A. Damme, R. D. Dewhurst, T. Kupfer, K. Radacki, K. Wagner, *J. Am. Chem. Soc.* **2011**, *133*, 19044–19047.
[22] Y. Wang, G. H. Robinson, *Inorg. Chem.* **2011**, *50*, 12326–12337.
[23] F. Dahcheh, D. Martin, D. W. Stephan, G. Bertrand, *Angew. Chem. Int. Ed.* **2014**, *53*, 13159–13163; *Angew. Chem.* **2014**, *126*, 13375–13379.
[24] A. D. Ledet, T. W. Hudnall, *Dalton Trans.* **2016**, *45*, 9820–9826.
[25] A. D. Ledet, E. W. Reinheimer, T. W. Hudnall, *J. Chem. Crystallogr.* **2022**, 10.1007/s10870-022-00950-4.
[26] C. Pranckevicius, J. O. C. Jiménez-Halla, M. Kirsch, I. Krummenacher, H. Braunschweig, *J. Am. Chem. Soc.* **2018**, *140*, 10524–10529.
[27] C. Pranckevicius, C. Herok, F. Fantuzzi, B. Engels, H. Braunschweig, *Angew. Chem. Int. Ed.* **2019**, *58*, 12893–12897; *Angew. Chem.* **2019**, *131*, 13025–13029.
[28] V. Lavallo, Y. Canac, C. Präsang, B. Donnadieu, G. Bertrand, *Angew. Chem. Int. Ed.* **2005**, *44*, 5705–5709; *Angew. Chem.* **2005**, *117*, 5851–5855.
[29] H. Nöth, S. Weber, *Z. Naturforsch.* **1983**, *38B*, 1460–1465.
[30] A. N. Price, G. S. Nichol, M. J. Cowley, *Angew. Chem. Int. Ed.* **2017**, *56*, 9953–9957; *Angew. Chem.* **2017**, *129*, 10085–10089.
[31] B. Glaser, E. Hanecker, H. Nöth, H. Wagner, *Chem. Ber.* **1987**, *120*, 659–661.
[32] I. Manners, P. Paetzold, *J. Chem. Soc. Chem. Commun.* **1988**, 183–185.
[33] M. Arrowsmith, J. I. Schweizer, M. Heinz, M. Härterich, I. Krummenacher, M. C. Holthausen, H. Braunschweig, *Chem. Sci.* **2019**, *10*, 5095–5103.
[34] M. Arrowsmith, S. Endres, M. Heinz, V. Nestler, M. C. Holthausen, H. Braunschweig, *Chem. Eur. J.* **2021**, *27*, 17660–17668.
[35] M. Arrowsmith, D. Auerhammer, R. Bertermann, H. Braunschweig, G. Bringmann, M. A. Celik, R. D. Dewhurst, M. Finze, M. Grüne, M. Hailmann, T. Hertle, I. Krummenacher, *Angew. Chem. Int. Ed.* **2016**, *55*, 14464–14468; *Angew. Chem.* **2016**, *128*, 14680–14684.
[36] D. K. Roy, I. Krummenacher, T. Stennett, C. Lenczyk, T. Thiess, E. Welz, B. Engels, H. Braunschweig, *Chem. Commun.* **2018**, *54*, 9015–9018.
[37] Y.-J. Lin, W.-C. Liu, Y.-H. Liu, G.-H. Lee, S.-Y. Chien, C.-W. Chiu, *Nat. Commun.* **2022**, *13*, article 7051.
[38] NMR-spectroscopic analysis of the crude product shows that **3** is the only boron-containing product formed. The poor isolated yield results from washing of the crude product with cold acetonitrile to remove leftover **2** and impurities.
[39] M.-A. Légaré, M. Rang, G. Bélanger-Chabot, J. I. Schweizer, I. Krummenacher, R. Bertermann, M. Arrowsmith, M. C. Holthausen, H. Braunschweig, *Science* **2019**, *363*, 1329–1332.
[40] H. Nöth, H. Vahrenkamp, *Chem. Ber.* **1966**, *99*, 1049–1067.
[41] M. Rang, F. Fantuzzi, M. Arrowsmith, E. Beck, R. Witte, A. Matler, A. Rempel, T. Bischof, K. Radacki, B. Engels, H. Braunschweig, *Angew. Chem. Int. Ed.* **2021**, *60*, 2963–2968; *Angew. Chem.* **2021**, *133*, 3000–3005.
[42] M.-A. Légaré, G. Bélanger-Chabot, R. D. Dewhurst, E. Welz, I. Krummenacher, B. Engels, H. Braunschweig, *Science* **2018**, *359*, 896–900.
[43] S. Kundu, S. Sinhababu, V. Chandrasekhar, H. W. Roesky, *Chem. Sci.* **2019**, *10*, 4727–4741.
[44] A. Stoy, J. Böhnke, J. O. C. Jimenéz-Halla, R. D. Dewhurst, T. Thiess, H. Braunschweig, *Angew. Chem. Int. Ed.* **2018**, *57*, 5947–5951; *Angew. Chem.* **2018**, *130*, 6055–6059.
[45] M. Arrowsmith, J. Böhnke, H. Braunschweig, M. A. Celik, *Angew. Chem. Int. Ed.* **2017**, *56*, 14287–14292; *Angew. Chem.* **2017**, *129*, 14475–14480.
[46] A. Hofmann, M.-A. Légaré, L. Wüst, H. Braunschweig, *Angew. Chem. Int. Ed.* **2019**, *58*, 9776–9781; *Angew. Chem.* **2019**, *131*, 9878–9883.
[47] C. Pranckevicius, C. Herok, F. Fantuzzi, B. Engels, H. Braunschweig, *Angew. Chem. Int. Ed.* **2019**, *58*, 12893–12897; *Angew. Chem.* **2019**, *131*, 13025–13029.
[48] D. Auerhammer, M. Arrowsmith, J. Böhnke, H. Braunschweig, T. Kupfer, *Chem. Sci.* **2018**, *9*, 2252–2260.
[49] S. Liu, M.-A. Légaré, A. Hofmann, H. Braunschweig, *J. Am. Chem. Soc.* **2018**, *140*, 11223–11226.
[50] S. Liu, M.-A. Légaré, A. Hofmann, A. Rempel, S. Hagspiel, H. Braunschweig, *Chem. Sci.* **2019**, *10*, 4662–4666.
[51] C. Shan, S. Yao, M. Driess, *Chem. Soc. Rev.* **2020**, *49*, 6733–6754.
[52] K. C. Mondal, P. P. Samuel, M. Tretiakov, A. P. Singh, H. W. Roesky, A. C. Stückl, B. Niepötter, E. Carl, H. Wolf, R. Herbst-Irmer, D. Stalke, *Inorg. Chem.* **2013**, *52*, 4736–4743.
[53] A. Das, B. J. Elvers, M. K. Nayak, N. Chrysochos, S. Anga, A. Kumar, D. K. Rao, T. N. Narayanan, C. Schulzke, C. B. Yildiz, A. Jana, *Angew. Chem. Int. Ed.* **2022**, *61*, e2022026.
[54] D. Männig, C. K. Narula, H. Nöth, U. Wietelmann, *Chem. Ber.* **1985**, *118*, 3748–3758.
[55] E. Hanecker, H. Nöth, U. Wietelmann, *Chem. Ber.* **1986**, *119*, 1904–1910.
[56] K. C. Mondal, P. P. Samuel, M. Tretiakov, A. P. Singh, H. W. Roesky, A. C. Stückl, B. Niepötter, E. Carl, H. Wolf, R. Herbst-Irmer, D. Stalke, *Inorg. Chem.* **2013**, *52*, 4736–4743.
[57] Heating the reaction to 60 °C did not improve the conversion and led to decreased selectivity.
[58] NMR shift calculations at the B3LYP-D3(BJ)-Def2-SVP level of theory predict an ^{11}B NMR shift of 46 ppm for **7**, using compound **2** (δ_{11B} = 71 ppm) as the reference.
[59] A Bondi, *J. Phys. Chem.* **1964**, *68*, 441–451.
[60] H. Wang, J. Zhang, H. Hu, C Cui, *J. Am. Chem. Soc.* **2010**, *132*, 10998–10999.
[61] K. Jaiswal, B. Prashanth, S. Ravi, K. R. Shamasundar, S. Singh, *Dalton Trans.* **2015**, *44*, 15779–15785.

Manuscript received: November 24, 2022
Accepted manuscript online: December 23, 2022
Version of record online: February 16, 2023